# Opportunities for sol–gel materials in fuel cells[*]

LISA C. KLEIN

Rutgers-the State University of New Jersey, Ceramic & Materials Engineering,
607 Taylor Road, Piscataway, NY 08854-8065, USA

Fuel cells are electrochemical devices that convert the chemical energy of a fuel and oxidant directly to electrical energy. Three types of fuel cells are (a) proton-exchange membrane fuel cells (PEMFC), (b) molten carbonate fuel cells (MCFC) and (c) solid oxide fuel cells (SOFC). In each case, there is a role for sol–gel processing. In the case of PEMFC, sol–gel modifications to the membrane are designed to increase the operating temperature. In the case of MCFC, sol–gel corrosion barriers extend the lifetime of the current collector. Finally, sol–gel processing is being used to assemble the electrolyte and electrode layers in SOFC and related oxygen generating devices. Examples are given for the application of sol–gel processing in each system, pointing out the derived benefits and areas for further development.

Key words: sol–gel materials processing, fuel cells, proton exchange, molten carbonate, solid oxide

## 1. Introduction

Fuel cells are electrochemical cells that convert the chemical energy of a fuel and an oxidant to electrical energy by a process involving an invariant electrode–electrolyte system [1]. Fuel cell systems are built for a wide range of power requirements from a few hundred watts to megawatts. Transportation fuel cells are being promoted for their high-energy efficiency and low emissions, compared to internal combustion engines. In addition, fuel cells are being developed for stationary applications, as back up generators and co-generation systems.

Sol–gel processing is finding its way into the fabrication of fuel cell components. Our interest is to find places where sol–gel processing offers either an advantage or unique capability. In some cases, sol–gel processing is a substitution for a conventional process, for example, where tape cast layers are used in a solid oxide fuel cell. In other cases, sol–gel processing offers a new approach, for example, where gel is incorporated into a polymer for a proton exchange membrane (also called polymer

_____

[*]The paper presented at the International Conference on Sol–Gel Materials, SGM 2001, Rokosowo, Poland.

electrolyte) fuel cell. The motivation for trying sol–gel processing is based on our previous use of sol–gel processing in other electrochemical devices, both lithium-ion batteries and electrochromic displays.

# 2. Previous use of sol–gel processing in electrochemical devices

## 2.1. Lithium ion batteries

Recall for a moment, the basic galvanic cell. The cell consists of an anode, a cathode and an electrolyte. In a lithium rechargeable battery, the cathode material is an intercalation compound with a layered or framework structure [2].

On charging the Li is oxidized at the cathode:

$$Li \rightarrow Li^+ + e \qquad (1)$$

and reduced at the anode

$$Li^+ + e \rightarrow Li \qquad (2)$$

In lithium batteries, sol–gel processing has been applied principally to the solid electrolyte [3].

The electrolyte is the critical feature in a galvanic cell, including fuel cells, because it has to transport ions back and forth between the cathode and anode. The electrolyte has to have a wide electrochemical potential window and stability during charge/overcharge and discharge/over-discharge. A solid electrolyte has to have mechanical stability. While it serves as a separator and membrane, it is also rigid, holding the components of the cell fixed.

One problem with solid electrolytes is that they may not have high ionic conductivity. One way around this problem is thin film electrolytes. A natural advantage of the sol–gel process is the fact that a film of oxide can be deposited directly from solution [4].

It is well known that ionic transport in solid electrolytes is an activated process, and the temperature dependence of ionic conductivity is represented by an Arrhenius-type equation with apparent activation energy. In most fast ion conductors, the activation energy is indicative of the energy of motion rather than the energy to form charge carriers. That is the population of mobile carriers is high and needs only to be set in motion. The desired features in a fast ion conductor are a large number of mobile ions, a large number of sites for the ions, relatively low activation energy, and ease of fabrication in complex shapes. Compared to crystalline fast ion conductors, sol–gel processed ion conductors, in particular lithium containing silicates, are isotropic, have more channels for fast ion conduction, and have fewer restrictions on composition [5].

## 2.2. Electrochromic devices

Another example of a galvanic cell is an electrochromic (EC) device, which is a multilayer construction where one of the layers shows electrochromic properties [6–8]. Certain compounds, especially oxides of polyvalent metals, exhibit coloration that depends on the oxidation state of their cations. This property leads to electrochromism, which is a reversible and visible change in transmittance. The oxidation–reduction reactions are electrochemically induced using low voltages, on the order $\pm 1$ V dc.

The most well known "chromogenic" material is tungsten trioxide ($WO_3$) forming deep blue alkali and hydrogen tungsten bronzes ($M_xWO_3$) on reduction. The reaction is expressed by the following equation:

$$\underset{\text{clear}}{W^{6+}O_3} + xM^+ + xe = M_xWO_3 = \underset{\text{blue}}{M_xW_x^{5+}W_{1-x}^{6+}O_3} \qquad (3)$$
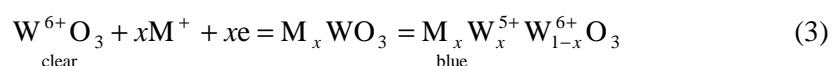
where M is hydrogen or alkali and $0 < x < 1$.

There are several approaches to the preparation of transition metal oxides [9]. One of the routes is to prepare a solution using alkoxides only. The available alkoxides are only slightly soluble in common organic solvents and are very reactive with water, making them difficult to handle. Another route is to use salts such as oxychlorides as the network former oxide precursor. The third route is to use colloidal sols. A sol, which is a colloidal suspension of small particles (1–1000 nm) in a liquid, is obtained after hydrolysis-condensation reactions of the precursor. The least expensive precursor is tungstic acid. Other reasons for choosing tungstic acid are its aqueous nature, its ability to be recycled, the presence of W–O–W bonds in the sols, and the absence of crystallinity. One drawback of tungstic acid sols is that they turn into a gel in 30 min.

For sol–gel electrolytes in electrochromic devices, the primary advantage is high lithium ionic conductivity [10]. Of course, the electrolyte has to have high electronic resistivity, high ionic conductivity, and no defects (pinholes). The commercially introduced devices have "no moving parts" meaning no mobile protons that will defeat the memory capability of the device [11].

For lithium batteries and electrochromic devices, sol–gel processing seems well suited. On the one hand, gels are inorganic and rigid, which means that the sol–gel electrolyte can operate at modest temperatures while playing the role of a mechanical divider between the electrodes. On the other hand, sol–gel processing is practical for large area coatings where sols can be applied directly to substrates and in successive sol–gel layers.

## 3. Use of sol–gel processing in fuel cells

Buoyed by the success of sol–gel processing in batteries and electrochromic devices, we have extended its use to other electrochemical devices and systems. Because

of the high interest in alternative power generation, fuel cells are a natural area for investigation.

### 3.1. Proton exchange membrane fuel cells (PEMFC)

Recent advances have made proton-exchange membrane fuel cells (PEMFC), a leading alternative to internal combustion and diesel engines for cars, trucks and buses. These advances include the reduction of the platinum electrode catalyst needed, and membranes with high specific conductivity, good water retention and long lifetimes [12]. A major limitation of the current PEMFC is that the Pt anode electrocatalysts is poisoned by CO at the 5 to 10 ppm level in the state-of-the-art fuel cells operating at about 80 °C [13, 14]. One approach to solving the CO poisoning problem is to operate at higher temperature where the free energy of adsorption of CO on Pt has a larger positive temperature dependence than that of $H_2$, which means that the CO tolerance level increases with temperature [15].

A complication in current PEMFC's is water management. The proton conductivity of the PEM (Nafion) increases linearly with the water content, with the highest conductivity corresponding to a fully hydrated membrane. While it is desirable to operate a fuel cell at a temperature above the boiling point of water from the standpoint of increased reaction kinetics and lower susceptibility to poisoning, the membranes lose conductivity due to drying. Membrane dehydration also causes the membrane to shrink, which reduces the contact between the electrode and membrane, leading to the crossover of the reactant gases. The problem is that the vapor pressure of water increases very rapidly with temperatures above 100 °C. In order to maintain the needed hydration for the polymeric membrane and the partial pressures of the reactant gases, the total pressure has to be increased significantly.

To solve both the CO poisoning and the water management problems, the present state-of-the-art PEM's need to be modified. One way to enhance the water retention of Nafion is incorporation of hydrophilic oxides (e.g. $SiO_2$). Difficulties have been encountered because the metal oxide particles are micron size and are not sufficiently small to enter the nanopore structure of the membrane [16]. To overcome this problem, a sol–gel technique has been used to introduce a polymeric oxide into the perfluorosulfonic acid membrane. Using this method, it was shown that the oxides enter the fine channels (~5 nm) [17].

Silicophosphate gels have been shown to be fast proton-conducting solids. The mobility of protons increases when the protons are strongly hydrogen-bonded. Compared with Si–OH, phosphate gels are better for high protonic conduction because the hydrogen ions are more strongly bound to the non-bridging oxygen. Also, the hydrogen in the P–OH group is more strongly hydrogen-bonded with water molecules, resulting in an increase in the temperature necessary to remove the water. The introduction of cations such as $Zr^{4+}$ into silicophosphate gels results in improved chemical stability [18, 19].

We prepared a sol of composition $60SiO_2–30P_2O_5–10ZrO_2$ sol using tetraethyl orthosilicate ($Si(OC_2H_5)_4$, TEOS), triethyl phosphate ($PO(OC_2H_5)_3$, TEP), and zirconium -*n*-propoxide ($Zr(OC_3H_7)_4$, TPZr). The sol was prepared by mixing two solutions. Solution A was prepared by mixing TEOS, half the volume of propanol (solvent), TEP, HCl (to control the pH at ~2) and water (molar ratio of water/(TEOS + TEP) = 2) at room temperature and stirred for 1 h. Solution B was prepared by mixing TPZr, the other half of the propanol and acetylacetone (molar ratio of acetylacetone/TPZr = 1) at room temperature and stirred for 1 h. Both solutions were subsequently mixed together and stirred for 1 h. The remaining water was added drop by drop, and then the solution was stirred for 15 min. The sol has a concentration of 70 grams of solid per liter, and a final molar ratio of water/precursors = 5.5.

The preparation of the infiltrated Nafion consisted of first pre-treating the Nafion membrane with 3 vol. % $H_2O_2$ for 2 hours at 80 °C, followed by 50 vol. % $H_2SO_4$ for 2 hours at 80 °C. The membrane was treated three times in distilled $H_2O$ at 80 °C to remove any excess acid. After drying for 3 days at 80 °C, the membrane was immersed in the $60SiO_2–30P_2O_5–10ZrO_2$ sol for 3 hours. Then, the membrane surfaces were cleaned with propanol to avoid the formation of surface-attached silicate layers. After the treatment, the membrane was placed at room temperature for 5 hours and then in an oven at 150 °C for 2 days. The dried infiltrated samples had an average weight increase of about 10%.

For the fuel cell experiments, the Pt/C fuel electrodes (ETEK Inc.) with a Pt loading of 0.4 mg·cm$^{-2}$, were impregnated with 0.6 mg·cm$^{-2}$ of Nafion (dry weight) by applying 12 mg·cm$^{-2}$ of 5% Nafion solution with a brush. The electrode area was 5 cm$^2$. The membrane electrode assembly (MEA) was prepared by heating the electrode/membrane/electrode sandwich to 90 °C for 1 minute in a Carver Hot-Press, followed by increasing the temperature to 130 °C for 1 minute and finally hot-pressing the MEA at 130 °C and 2 MPa for 1 minute. The MEA was positioned in a single cell test fixture, which was then installed in a fuel cell test station (Globetech Inc., GT-1000). The test station was equipped for the temperature-controlled humidification of the reactant gases ($H_2$, $O_2$ and air) and for the temperature control of the single cell.

For the performance evaluation of the PEMFC, the single cell was fed with humidified $H_2$ and $O_2$ at atmospheric pressure (reactant gas and water vapor pressure equal to 1 atm) and the temperature of the $H_2$ and $O_2$ humidifiers and of the single cell was raised slowly to 90 °C, 88 °C and 80 °C respectively. During this period, the external load was maintained at a constant value of 0.1 ohm, to reach an optimal hydration of the membrane using the water produced in the single cell. After the single cell had reached stable conditions (i.e. current density remained constant over time at a fixed potential), cyclic voltammograms were recorded at a sweep range of 20 m·V·s$^{-1}$ and in the range of 0.1 V to 1 V vs. reversible hydrogen electrode (RHE) for one hour. Cell potential vs. current density measurements were then made at a relative humidity of 90–100%. The flow rates of gases were two times stoichiometric.

This study was carried out to know whether or not the incorporation of $SiO_2$–$P_2O_5$–$ZrO_2$ gel in Nafion enhances the current density at a fixed potential, for temperatures > 130 °C. By limiting the total pressure to 3 atm, the maximum operating temperature investigated was 140 °C since the vapor pressure of water at this temperature is 3.5 atm. In fact, we measured a significant improvement in the water management of the composite vs. the control Nafion membrane. The higher current densities and lower resistances of the composite membrane can be attributed to the water retention characteristic of the $SiO_2$–$P_2O_5$–$ZrO_2$ gel. In addition, composite membranes were less susceptible to high temperature loss of proton conductivity than unmodified Nafion. These promising results are being investigated further [20].

### 3.2. Molten carbonate fuel cells (MCFC)

Another fuel cell design is the molten carbonate fuel cell (MCFC) [21], which operates in the temperature range 620–660 °C with an efficiency of > 50%. MCFC units are produced by FuelCell Energy, Inc (Danbury, CT). These units are designed as back-up generators for intermittent use. The operational lifetimes of fuel cell systems need to be extended. In order to do so, it is necessary to limit component corrosion.

Corrosion of the lithiated NiO cathode and corrosion of the 316L stainless steel cathode current collector shorten the useful lifetime of an MCFC. The long-term performance of fuel cells depends on their resistance to degradation in an aggressive environment. The electrode reactions are:
- anode (Ni):

$$H_2 + CO_3^{2-} \rightarrow H_2O + CO_2 + 2e \qquad (4)$$

- cathode (NiO):

$$\frac{1}{2}O_2 + CO_2 + 2e \rightarrow CO_3^{2-} \qquad (5)$$
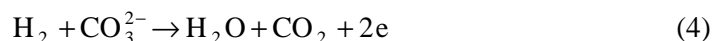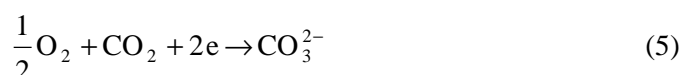
in a typical electrolyte of 62 mol % $Li_2CO_3$–38 mol % $K_2CO_3$ at an operating temperature of 650 °C in an atmosphere containing CO, $CO_2$, $O_2$, $H_2$, and $H_2O$.

During operation, the stainless steel cathode current collector forms a surface oxide, which increases the cathode/cathode current collector resistance. In addition, the surface oxide can react with the electrolyte to form $LiFeO_2$ and $K_2CrO_4$. Hot corrosion accelerates electrolyte loss, which can cause electrode performance decay, matrix ionic resistance increase, and reactant crossover increase [22, 23]. One way to control the surface oxide formation and limit its undesirable effect is to coat the current collector, with oxides such as $Li(Co,Fe)O_2$ [24] .

We have prepared aqueous coatings that (1) adhere to the 316L stainless steel cathode current collector, (2) crystallize during heat treatment, (3) remain intact on

the current collector at the operating temperature of the fuel cell (650 °C), and (4) provide protection without interfering with the operation of the current collector.

The starting materials were soluble salts, cobalt acetate ($Co(C_2H_3O_2)_2 \cdot H_2O$) and iron nitrate ($Fe(NO_3)_2 \cdot 9H_2O$). These salts produce hydroxides ($M(OH)_2$), oxyhydroxides ($MOOH$) or hydrated oxides in water, where M is Co or Fe. These solutions were reacted with lithium hydroxide. Diluted ammonium hydroxide (3M) was added to form stable colloids [25].

Lithium hydroxide and cobalt acetate were dissolved separately in distilled water. These two solutions were then mixed together and stirred vigorously. The hydrolysis of the mixture was promoted by slow addition of 3M ammonium hydroxide. Similarly, sols with ferric nitrate, or ferric nitrate plus cobalt acetate, were prepared. The sols used for coating were diluted to give a 2:1 ratio of moles water to moles oxide.

The sols were coated onto 316L stainless steel substrates using a dip-coating technique. As the surface of the substrates was somewhat rough, the samples were polished and cleaned before coating. The substrates were put into a boiling sodium carbonate/water solution to remove oil and grease, then rinsed in water, and put into a mixture of $HCl/HNO_3$ to remove rust and increase the activity of the surface. The substrates were rinsed again in water followed by ethanol, and dried in an oven.

During the dip-coating process, the substrates were immersed in the sol for about one minute, and then withdrawn at a speed of about 2 mm/min. After coating, the samples were put into the dryer at 100 °C and stored there until further heat treatment. After storing for up to 10 hr, the samples were heated to 650 °C for 3 hours, at a heating rate of 10 °C/min.

XRD patterns were collected from the powders of lithium cobalt oxide coatings scraped off of the substrate after heat treatment at several temperatures between 100 and 650 °C. Below 350 °C, no compounds were identified, although the diffraction patterns showed some small peaks. The first crystalline phases appeared at 350 °C, and the peaks were sharp by 550 °C. Principally, two crystalline phases exist which matched $Li_{1.47}Co_3O_4$ and a minor amount of $LiFe_5O_8$. The minor phase resulted from the reaction between coating and substrate.

The XRD pattern of the powders scraped off of the substrate with nominal composition $LiFeO_2$ matched the pattern for $LiFe_5O_8$. The coatings containing Co and Fe showed complex patterns with peaks from both the $LiCoO_2$ system and $LiFeO_2$ system.

Table 1. Coating compositions, thickness
and transformation temperatures (determined by DSC)

| Nominal composition | Thickness/m | Transformation temperature/°C |
|---|---|---|
| $LiCoO_2$ | 2.8 | 370–410 |
| $LiCo_{0.5}Fe_{0.5}O_2$ | 1.2 | 225 |
| $LiFeO_2$ | 1.2 | 270 |

Thermal cycling tests were carried out for $LiCoO_2$ coatings. The cycling was from room temperature to 650 °C for 10 cycles with a heating rate and cooling rate of 600 °C/h and a dwell time of 0.1 hr at RT and 650 °C. This cycle was used as a simulation of how the fuel cell may be used. The microhardness was measured before and after cycling and showed little change [26]. Also, a comparison of SEM micrographs before and after thermal cycling showed the microstructures are similar. There were no obvious cracks after thermal cycling, which suggests thermal compatibility between the coating and the 316L stainless steel substrate.

## 4. Oxygen generators

The ceramic oxygen generator is based on oxygen ion conducting technology. Its functioning is very similar to solid oxide fuel cells (SOFC). The oxygen generators that can be found in industry are usually based upon pressure swing adsorption (PSA) technology. Although they are extremely reliable, these systems have certain limitations. The purity of the oxygen is only about 95%. They require auxiliary equipment, such as inlet compressors, activators for nitrogen adsorption tanks, and the adsorbent can become ineffective when exposed to contaminated air or excess humidity.

Compared to PSA technology, ceramic oxygen generators have many advantages. The purity of the oxygen is higher (99.9%). Potentially, the size is smaller, and it is less noisy. These devices are needed for portable oxygen supplies to remote hospitals, portable welding platforms, manned space programs, and breathing air purification against contaminants such as biological agents.

An electrochemical device for oxygen generation, similar to SOFC, requires three successive layers. First, the cathode layer also serves as a catalyst for the reduction of oxygen in air. An oxygen ion-conducting layer is the electrolyte. Last, an anode layer needs to recombine the oxygen ions in $O_2$. The basic operation of the oxygen generator is to make oxygen pass through an oxygen ion conducting membrane by applying a potential. Typically, an oxygen generator or SOFC operates at about 800 °C. Air diffuses through the porous cathode, usually $La_{1-x}Sr_xMnO_3$ (LSM), to the cathode/solid electrolyte interface where the oxygen is reduced:

$$\text{cathode/electrolyte: } O_2 + 4e \rightarrow 2O^{2-} \tag{6}$$
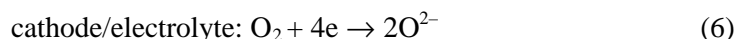
The resulting oxygen ions cross the electrolyte under the influence of the electric field, and reach the electrolyte/anode interface. The opposite reaction of oxidation occurs, and the reformed oxygen proceeds outward through the porous anode.

$$\text{electrolyte/anode: } 2O^{2-} \rightarrow O_2 + 4e \tag{7}$$
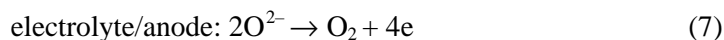
The driving force for the diffusion of the oxygen ions is the difference of potential imposed by the applied voltage. Moreover, the ceramic solid electrolyte has infinite selectivity, since no gas except oxygen can cross the cell [27].

The performance of the oxygen generator depends mainly on two parameters, the current density at a given cell dc potential and the Faradaic efficiency. The current density is the amount of current that passes through a unit active area of the cell. For a commercial oxygen generator, the current density has to be at least 100 mA·cm$^{-2}$.

The second parameter, the Faradaic efficiency, is a measure of the amount of current passing through an oxygen generator cell. For an oxygen generator operating at ambient pressure 1 atm and 800 °C, the Faradaic efficiency is 13.7 cm$^3$ (min·A)$^{-1}$ when all the current is due to the oxygen ion transport. The Faradaic efficiency is then said to be 100%.

The high operating temperature leads to complex materials problems, such as interfacial diffusion, electrode sintering, and mechanical stress. In order to reduce the operating temperatures, the resistive loss occurring in the electrolyte should be minimized. One of the solutions is to decrease the thickness of the solid electrolyte from several hundred micrometers, the usual thickness in conventional cells, to a range close to ten micrometers. Among the different methods to deposit thin films, here again is an opportunity for the sol–gel process. In addition, sol–gel synthesized layers sinter at low temperature [28].

Lanthanum manganite doped with strontium (LSM) is used as the cathode material. It is also used as the anode. The solid electrolyte is yttrium-stabilized zirconia (YSZ), one of the best oxygen ion conductors at high temperature. To compensate the positive charge deficit induced by the substitution of $Zr^{4+}$ ions by $Y^{3+}$ ions, vacancies are created on the oxygen lattice. Moving from vacancy to vacancy, oxygen ions can diffuse through the material. Although the YSZ coating has to be thin to be an efficient ionic conductor, it remains a rigid gas separator and an electronic insulator. Platinum paste is used at the connection between the power supply and the oxygen generator.

A sol–gel process can be used for all the coatings. LSM for the cathode is at first deposited on a substrate. The YSZ for the electrolyte is then coated on the cathode. Finally LSM for the anode is deposited on the YSZ.

### 4.1. Yttria-stabilized zirconia (YSZ)

Due to its excellent properties as an oxygen ionic conductor, yttria-stabilized zirconia (YSZ) has been studied widely [29]. YSZ is a popular electrolyte in solid oxide fuel cells (SOFC) and is used in applications designed for oxygen separation from air.

Zirconia gels doped with yttria were prepared as follows: 60 ml of zirconium oxychloride was diluted in a mixture of water plus ethanol (1:1 by volume). Then yttrium nitrate solution (10 mole %) was added. The solution was mixed and heated up to 80 °C and then 50 ml of 1.5 M $NH_4OH$ was added to promote the condensation of the species. A homogeneous white sol was obtained.

The YSZ sol, with a viscosity of about 100 cps, was applied with a brush to a platinum coated ceramic substrate. Several coatings were applied on top of each

other to build a thick enough layer. Each coating was heat-treated to 1100 °C for 5 minutes at a heating rate of 500 °C per hour to remove the organic species and to sinter this coating together with the previous one. A final heat treatment to 1200 °C at a heating rate of 500 °C per hour is done as a final sintering step.

All the samples have the stabilized cubic phase. No second phases, tetragonal zirconia or yttria oxide, were detected. The densification temperature was lower than that in the solid-state preparation where zirconia powders are reacted with yttria powder. With sol–gel processed YSZ, residual porosity is removed after firing at 900 °C for five hours [30].

The thickness increases almost linearly with the number of coatings greater than 15, with each coating contributing to approximately 0.5 micron thickness. With fewer than 30 coatings, the YSZ layers are not gas tight, but with 40 or more coatings, the YSZ can retain pressures of a few atmospheres.

For the sol–gel YSZ, both the bulk and the boundary conductivities increase with the length of the sintering heat treatment. Usually, in conventional powders, bulk conductivity is not affected by the sintering conditions, whereas the grain boundary conductivity is [31]. However, the sol–gel YSZ may experience some further densification and grain growth under the conditions of heat treatment [32, 33].

In summary, the sol–gel route to process YSZ electrolyte leads to dense and thin layers (about 20 microns) whose thickness can be controlled by the number of applied coatings. A minimum number of coatings are required to obtain gas-tight layers, due to the presence of microstructural defects on the outer surface. The conductivity of the YSZ layers improves with the length and the number of heat treatments, which promote further densification of the oxide. However, the conductivity is still lower than reported for conventional powder processing [34]. The lower values result from inhomogeneities in the microstructure remaining when all the coatings do not receive the same number of heat treatments. Nevertheless, those defects may play a role when applying the LSM gel coatings on top of the YSZ layer, since they enable the formation of an intermediate electrode/electrolyte mixed area, which reduces the interfacial voltage drop.

## 4.2. Lanthanum strontium manganite (LSM)

Several properties of the lanthanum manganite doped with strontium recommend it as an electrode for the oxygen generator. First of all, $La_{1-x}Sr_xMnO_3$ is a good electronic conductor. To compensate the decrease of positive charge due to the substitution of $La^{3+}$ cations by $Sr^{2+}$ cations, some manganese cations change their degree of oxidation from 3+ to 4+. The electrons can hop between the $Mn^{3+}$ and $Mn^{4+}$. The electronic conductivity increases when the content of doping ions increases, because the concentration in $Mn^{4+}$ ions increases. LSM is known to exhibit a semiconductor behavior for $x \geq 0.5$ and a metallic behavior for $x \leq 0.5$ [35, 36]. LSM is also an oxygen ion conductor, so a charge transfer from the bulk enhances its electrocatalytic

activity. The number of oxygen vacancies in $La_{1-x}Sr_xMnO_3$ is assumed to be close to zero when $x = 0.5$.

In the present investigation, $x = 0.33$ to achieve a high electrical conductivity, high electrocatalytic activity, and a thermal expansion compatible with YSZ. Several low temperature synthesis routes, based on solution chemistry methods, have used to prepare LSM. First, the so-called Pechini, process mixes a hydrocarboxylic acid (often citric acid) and a poly(hydroxyl alcohol) (usually ethylene glycol) with the cation salts dissolved in water. After a short time at about 100 °C, polyesterification occurs, homogeneously distributing the cations throughout the polymer. The common cation salts are nitrates [37, 38], carbonates [39], chlorides or hydroxides [40].

$La_{0.66}Sr_{0.33}MnO_3$ was prepared with lanthanum nitrate, lanthanum acetate and lanthanum chloride. After dissolution in water, they were mixed with manganese acetate and strontium nitrate, and then stirred for half an hour. A gel formed after addition of citric acid which protonates the ligands. Ethylene glycol was used for esterification and to improve solubility. Finally ammonium hydroxide was added for peptization, followed by stirring for one hour.

Within two days at 50 °C, the gels made with the $La(NO_3)_3$ and $La(CH_3COO)_3$ were completely dried, whereas the one made with $LaCl_3$ only turned into a stiff, transparent cake. All gels then were dried at 80 °C for one day. The powders obtained after grinding were heated up to 1100 °C.

Pure LSM is observed on the XRD patterns of the powder heated at 770 °C and 1100 °C for one hour. The symmetry of the perovskite is the same for all three La-precursors, rhombohedral. The various structures of the manganite are well known [41]. The perovskite symmetry is largely determined by the concentration of $Mn^{4+}$ cations. $Mn^{4+}$ cations are smaller than $Mn^{3+}$ cations, and their substitution leads to lattice shrinkage. In undoped manganite, the excess of oxygen atoms in the lattice controls the concentration of $Mn^{4+}$. The crystal structure depends strongly on the preparation procedure, especially the firing temperature and atmosphere. In contrast, the level of substitution fixes the concentration of $Mn^{4+}$ cations. The temperature dependence of the conductivity is linear with a slight negative slope. While the bulk conductivity in this composition should be electronic, it appears that the small grain size and large grain boundary area are controlling the conductivity of the LSM porous electrodes [42,43]. The activation energies for samples prepared with the nitrate were lower than those prepared with the chloride or acetate, suggesting the lanthanum nitrate is the preferred lanthanum precursor for the electrodes.

Finally, the thermal expansion characteristics of $La_{0.66}Sr_{0.33}MnO_3$ and YSZ are well matched. The match is simplified because the electrode is porous, that is the contact areas between the LSM and the YSZ are small. Moreover, LSM presents a high catalytic activity for the reduction of the oxygen molecules. The major part of the oxygen ions that enter the electrolyte vacancies comes from reactions of dissociation and ionization of oxygen molecules at the Triple Phase Boundary (TPB). As its name indicates, the three phases are present in this zone located at the electrode/electrolyte interface: air, electrolyte and cathode. Starting with the oxygen

molecule and ending with the transport of oxygen ions in the electrolyte, adsorption of the molecule on the surface of the electrode, dissociation of the adsorbed molecule and finally ionization of the adsorbed atoms are all required.

In addition, LSM has good mechanical properties and long-term stability at 800 °C. It is chemically inert toward the surrounding gas, and it is chemically compatible with the YSZ, even though small amounts of undesirable phases, like $La_2ZrO_7$ or $SrZrO_3$, appear at the interface, increasing slightly the overpotential [44].

In summary, the efficiency of the oxygen generator depends on its microstructure. The LSM electrode material has to be porous and to have a small particle size to optimize the active surface area at the TPB. At the same time, the YSZ electrolyte has to be dense and air tight. Both have to reach their final microstructure in one final heat treatment at 1200 °C in order to produce the working device. Sol–gel processing is the key to assembling the consecutive layers.

# 5. Conclusions

In conclusion, sol–gel processing has been used to prepare a number of complex oxide compositions. By using the sol–gel process, components that appear in fuel cells have been fabricated. These examples show the advantages of sol–gel processing for (1) forming hybrids with polymers, (2) depositing thin films in consecutive layers, and (3) creating layers that densify at temperatures below 1200 °C.

## Acknowledgements

## References

[1] KORDESCH K., SIMADER G., *Fuel Cells and Their Applications*, 1996, New York, VCH, Weinheim.
[2] BARBOUX P., TARASCON J.M., SHOKOOHI F.K., J. Solid State Chem., 1991, 94, 185.
[3] KLEIN L.C., HO S.F., SZU S-P., GREENBLATT M., [in:] *Applications of Analytical Techniques to the Characterization of Materials*, D.L. Perry (Ed.), 1991, Plenum Press, New York, p. 101.
[4] BRINKER C.J., HURD A.J., FRYE G.C., SCHUNK P.R., ASHLEY C.S., [in:] *Chemical Processing of Advanced Materials*, L.L. Hench and J.K. West (Eds.), 1992, New York, Wiley, p. 395.
[5] BOILOT J.P., COLOMBAN PH., [in:] *Sol–gel Technology for Thin Films, Fibers, Preforms, Electronics and Specialty Shapes*, L.C. Klein (Ed.), 1988, New York, Noyes Publication, p. 303.
[6] BAUCKE F.G.K., Materials Science and Engineering, 1991, B10, 285.
[7] GREENBERG C.B., Thin Solid Films, 1994, 251, 81.
[8] GRANQVIST C.G., Electrochimica Acta, 1999, 44, 3005.

[9] LIVAGE J., [in:] *Solid State Ionics III*, G-A. Nazri, J. M. Tarascon and M. Armand (Eds.), MRS 293, 1993, Pittsburgh PA, p. 261.

[10] MOUCHON E., KLEIN L.C., PICARD V., GREENBLATT M., [in:] Better Ceramics Through Chemistry VI, Eds. A. Cheetham, C.J. Brinker, M.L. Mecartney, C. Sanchez, MRS, 1994, 346, 189.

[11] CRONIN J.P., TARICO D.J., TONAZZI J.C.L., AGRAWAL A., KENNEDY S.R., Solar Energy Materials and Solar Cells, 1993, 29, 371.

[12] WAKIZOE M., VELEV O.A., SRINIVASAN S., Electrochimica Acta, 1995, 40, 335.

[13] LEE S.J., MURKERJEE S., TICIANELLI E.A., MCBREEN J., Electrochimica Acta, 1999, 44, 3283.

[14] DENIS M.C., LALANDE G., GUAY D., DODELET J.P., SCHULZ R., J. Applied Electrochemistry, 1999, 29, 951.

[15] KREUER K.D., Solid State Ionics, 1997, 97, 1.

[16] ANTONUCCI P.L., ARICO A.S., CRETI P., RAMUNNI E., ANTONUCCI V., Solid State Ionics, 1999, 125, 431.

[17] MAURITZ K.A., Materials Science and Engineering, 1998, C6, 121.

[18] NOGAMI M., MIYAMURA K., ABE Y., J. Electrochemical Society, 1997, 144, 2175.

[19] NOGAMI M., NAGAO R., CONG W., ABE Y., Journal of Sol–Gel Science & Technology, 1998, 13, 933.

[20] APARICIO M., KLEIN L.C., ADJEMIAN K., BOCARSLY A., [in:] *Ceramic Transactions: Materials for Electrochemical Energy Storage and Conversion*, A. Manthiram, G. Ceder, P.N. Kumta, S.K. Sundaram (Eds.), American Ceramic Soc., Westerville OH, 2001.

[21] YUH C., JOHNSEN R., FAROOQUE M., MARU H., J. Power Sources, 1995, 56, 1.

[22] BIENDENKOPF P., SPIEGEL M., GRABKE H.J., Materials and Corrosion, 1997, 48, 731.

[23] MURAI M., TAKAZAWA K., SOEJIMA K., SOTOUCHI H., J. Electrochemical Soc., 1996, 143, 2481.

[24] MAKKUS R.C., HEMMES K., DEWIT J.H.W., J. Electrochemical Soc., 1994, 141, 3429.

[25] BARBOUX P., TARASCON J.M., SHOKOOHI F.K., J. Solid State Chemistry, 1991, 94, 185.

[26] CHEN W., KLEIN L.C., HUANG C., J. Sol–Gel Science & Technology, 2001, 27, 203.

[27] MINH N.Q., J. Am. Ceram. Soc., 1993, 76, 566.

[28] OKUBO T., NAGAMOTO H., J. Mater. Sci., 1995, 30, 749.

[29] WEN T.L., HERBERT V., VILMINOT S., BERNIER C., J. Mater. Sci., 1991, 26, 3787.

[30] OKUBO T., NAGAMOTO H., J. Mater. Sci., 1995, 30, 749.

[31] BADWAL S.P.S., DRENNAN J., J. Mater. Sci., 1987, 22, 3231.

[32] SCHOULER E.J.L., MESHABI M., VITTER G., Solid State Ionics, 1983, 9, 10, 989.

[33] VERKERK M.J., MIDDELHUIS B.J., BURGRAAF A.J., Solid State Ionics, 1982, 6, 159.

[34] GIBSON I.R., DRANSFIELD G.P., IRVINE J.T.S., J. Mater. Sci., 1998, 33, 4297.

[35] HAMMOUCHE A., SCHOULER E.J.L., HENAULT M., Solid State Ionics, 1988, 28, 30, 1205.

[36] TAKEDA Y., SAKADI Y., ICHIKAWA T., IMANISHI N., YAMAMOTO O., MORI M., MORI N., ABE T., Solid State Ionics, 1994, 72, 257.

[37] MAURIN I., BARBOUX P., LASSAILLY Y., BOILOT J.P., Chem. Mater., 1998, 10, 1727.

[38] CARTER S., SELCUK A., CHATER R.J., KAJDA J., KILNER J.A., STEELE B.C.H., Solid State Ionics, 1992, 53, 56, 597.

[39] KUO J.H., ANDERSON H.U., J. Solid State Chemistry, 1989, 83, 52.

[40] LESSING P.A., Ceramic Bulletin, 1989, 68, 1002.

[41] HAMMOUCHE A., SIELBERT E., HAMMOU A., Mat. Res. Bull., 1989, 24, 367.

[42] KERTESZ M., RIESS I., TANNHAUSER D.S., LANGPAGE R., ROHR F.J., J. Solid State Chemistry, 1982, 42, 125.

[43] KUO J.H., ANDERSON H.U., SPARLIN D.M., J. Solid State Chemistry, 1990, 87, 55.

[44] BRUGNONI C., DUCATI U., SCAGLIOTTI M., Solid State Ionics, 1995, 76, 177.